IOPscience iopscience.iop.org

Home Search Collections Journals About Contact us My IOPscience

Multiple scattering and the BGK Boltzmann equation

This article has been downloaded from IOPscience. Please scroll down to see the full text article.

2000 J. Phys. A: Math. Gen. 33 3137

(http://iopscience.iop.org/0305-4470/33/16/307)

View the table of contents for this issue, or go to the journal homepage for more

Download details:
IP Address: 171.66.16.118
The article was downloaded on 02/06/2010 at 08:05

Please note that terms and conditions apply.

J. Phys. A: Math. Gen. **33** (2000) 3137–3160. Printed in the UK PII: S0305-4470(00)11117-5

Multiple scattering and the BGK Boltzmann equation

G M Webb†, M Pantazopoulou† and G P Zank‡
† Lunar and Planetary Laboratory, University of Arizona, Tucson, AZ 85721, USA
‡ Bartol Research Institute, University of Delaware, Newark, DE 19716, USA

Received 18 January 2000

Abstract. A multiple scattering formalism is developed for the BGK Boltzmann equation. The formalism is equivalent to constructing the Neumann series for the corresponding integral equation. By using Laplace and Fourier transform methods, the distribution of unscattered particles f_0, and the distribution of particles that have undergone n-scatters, f_n ($n \geqslant 1$), are determined for the initial value problem in a uniform background medium. The relationship between the Green function solutions obtained by Fedorov and Shakhov (Fedorov Yu I and Shakhov B A 1993 *Proc. 23rd Int. Cosmic Ray Conf. (Calgary)* vol 3 p 215), Kota (Kota J 1994 *Astrophys. J.* **427** 1035) and Fedorov *et al* (Fedorov Yu I *et al Astron. Astrophys.* **302** 623–34), in studies of coherent and diffusive transport of energetic charged particles in the interplanetary medium and the multiple scattering series is elucidated. The multiple scattering approach yields results on the number of particles that have done n-scatters ($n \geqslant 1$). This information is not accessible in the Green function solutions given by Fedorov and Shakhov and Fedorov *et al* in references given above.

1. Introduction

The BGK Boltzmann equation has been used to study various aspects of cosmic ray transport in astrophysical settings. These include the derivation of diffusive transport equations for cosmic rays that generalize the diffusive cosmic ray transport equation (Parker 1965, Gleeson and Axford 1967, Dolginov and Toptygin 1967) to include cosmic ray viscosity and accelerating reference frame effects (Berezhko and Krymsky 1981, Earl *et al* 1988, Webb 1989); models of coherent and non-diffusive particle transport (Fisk and Axford 1969, Fedorov and Shakhov 1993, Kota 1994, Fedorov *et al* 1995); and nonlinear, one fluid models of cosmic ray modified shocks (Berezhko *et al* 1983). The BGK Boltzmann equation in one Cartesian space dimension is equivalent to the equation of radiative transfer (e.g., Chandrasekhar 1950, Case and Zweifel 1967). Similar equations also occur in neutron transport theory (Weinberg and Wigner 1958, Case and Zweifel 1967).

The main aim in this paper is to provide a detailed description of the role of multiple scattering in the time-dependent Green function solution of the BGK Boltzmann equation, in one Cartesian space dimension, in a uniform background medium obtained by Fedorov and Shakhov (1993) and Fedorov *et al* (1995). This solution is clearly of interest in radiative transfer theory, and was used by Fedorov and co-workers in studies of solar cosmic ray transport in the interplanetary medium. However, it should be noted at the outset, that the solution is highly idealized, and of limited applicability in the solar cosmic ray transport context. Kota (1994) obtained similar, idealized solutions for generalized BGK Boltzmann models with two different scattering times τ_1 and τ_2. The scattering time τ_1 describes particle scattering in the same hemisphere in velocity space (either the backward or forward hemisphere), whereas τ_2

0305-4470/00/163137+24$30.00 © 2000 IOP Publishing Ltd

describes the scattering of particles from one hemisphere to the other hemisphere. The case $\tau_2 \gg \tau_1$ in this model resembles highly anisotropic pitch angle scattering in which particles are scattered slowly through $\theta = 90^\circ$ pitch angle compared with scattering at other pitch angles. Kota showed that coherent particle pulses could be obtained in BGK Boltzmann models, provided the two scattering times τ_1 and τ_2 were not equal (pronounced coherent pulses were obtained if $\tau_2 \gg \tau_1$). A brief account of the multiple scattering description of the Fedorov and Shakhov (1993) solution is given in Webb *et al* (1999). The solution of the BGK Boltzmann equation for three-dimensional geometry, with instantaneous particle injection at $\boldsymbol{r} = 0$ was obtained by Fedorov *et al* (1996).

The simplest model problem in a cosmic ray transport context, is the case of energetic charged particle transport along a constant background magnetic field $\boldsymbol{B} = B_0 \boldsymbol{e}_x$, directed along the x-axis, in which the particles undergo magnetostatic scattering. In this case, the energetic particle distribution function $f(x, t; v, \mu)$ satisfies the Fokker–Planck equation:

$$\frac{\partial f}{\partial t} + v\mu \frac{\partial f}{\partial x} = \frac{\partial}{\partial \mu}\left(\frac{1-\mu^2}{2}\nu \frac{\partial f}{\partial \mu}\right) \equiv \left(\frac{\delta f}{\delta t}\right)_c^{(D)} \tag{1.1}$$

where $\nu = \langle (\Delta\theta)^2/\Delta t\rangle$ is the scattering frequency for particles with pitch angle θ and pitch angle cosine $\mu = \cos\theta$ associated with waves or turbulence in the background flow (e.g. Jokipii 1966, Skilling 1975). In (1.1), x and t denote the particle position and time t, and v denotes the particle speed. More complete versions of the particle transport equation (1.1), taking into account a non-relativistically moving background medium with velocity $\boldsymbol{V}(\boldsymbol{x}, t)$, adiabatic focusing, and energy changes due to compression or expansion, and acceleration of the background flow, and second-order Fermi acceleration due to counter propagating Alfvén waves are given by Skilling (1975). Cross field diffusion and particle drifts (e.g. Jokipii *et al* 1977) are neglected in (1.1). The BGK Boltzmann collision operator

$$\left(\frac{\delta f}{\delta t}\right)_c^{(\mathrm{BGK})} = \frac{\langle f\rangle - f}{\tau} \tag{1.2}$$

is sometimes used instead of the small-angle scattering collision term $(\delta f/\delta t)_c^{(D)}$ used in (1.1) (e.g. Earl *et al* 1988, Webb 1989). In general, this is not justified in the cosmic ray transport context, but it can be justified if one is only interested in a diffusion approximation description at late times. In (1.2), the angular brackets on $\langle f\rangle$ denote an average of f over μ. The BGK Boltzmann collision term in (1.2) represents isotropic, large-angle scattering.

Both the Fokker–Planck description, using the pitch angle diffusion collision term in (1.1) and the BGK collision term (1.2) lead to similar spatial diffusion equations describing the particle transport at late times after the particles have undergone many scatters. The diffusion approximation assumes that the pitch angle anisotropies are small, and that the length and timescales for the variation of $\langle f\rangle$ are much larger than the particle mean free path and collision time respectively (e.g. Jokipii 1966, Hasselmann and Wibberenz 1970). The diffusion equation description is not valid at early times, since the diffusion equation is non-causal, and has an infinite speed for the propagation of disturbances. Telegraph equation descriptions (e.g. Fisk and Axford 1969, Earl 1974a, b, Gombosi *et al* 1993, Pauls *et al* 1993) obtained by truncating the eigenfunction moment equations include the effects of the particle inertia, and result in models with a finite propagation speed for particle disturbances and incorporate diffusive-type behaviour at late times. In general, telegraph equation models do not adequately describe large anisotropies at early times, but they do provide an improvement over the non-causal diffusion equation description if the particle anisotropies are small.

Coherent particle pulses occurring in interplanetary observations (Lin 1970) can only be obtained if there is a small rate of particle scattering through the 90° pitch angle region of phase space. Coherent pulses do not occur if the scattering is isotropic (Earl 1993). Earl (1993) has developed both Monte Carlo simulations and eigenfunction moment equations to describe coherent particle transport (see also, Earl 1974a, b, 1989). Numerical codes (Kota *et al* 1982, Ng and Wong 1979, Ruffolo 1991) have been used to investigate the particle pitch angle evolution with application to the transport of solar cosmic rays in the interplanetary medium. Zank *et al* (1999) have developed Legendre polynomial expansion solutions of the BGK Boltzmann equation that can deal with both anisotropic distributions at early times, and nearly isotropic, diffusive-type behaviour at late times. Scattering eigenfunction expansion methods were used by Kirk and Schneider (1987a) to investigate the transport and acceleration of energetic particles at relativistic shocks where the particle pitch angle anisotropies can be large. Kirk and Schneider (1987b) carried out further studies of particle acceleration at relativistic shocks using Monte Carlo methods.

In section 2, the BGK Boltzmann equation and model are introduced. Section 3 reformulates the BGK Boltzmann equation as an integral equation in which the distribution at time t depends on the particle distribution function at the last scatter, and on the initial conditions. The multiple scattering series in this development is related to the Neumann series obtained from the iterates of the integral equation. Section 4 describes solutions of the BGK Boltzmann equation in Laplace–Fourier transform space. The Green function $\tilde{G}_c$ for the scattered particles, and the Green functions $\{\tilde{G}_n\}$ of particles that have done n-scatters are first obtained in Fourier–Laplace space (section 4) and the corresponding solutions in (x, t)-space are then obtained by Fourier–Laplace inversion (section 5). The Fedorov–Shakhov solution is obtained by summing the multiple scattering series. Numerical examples illustrating the Fedorov–Shakhov solution, and the multiple scattering approximation are developed in section 6. Section 7 concludes with a summary and discussion.

2. Model and equations

Our main interest in this paper is with solutions of the BGK Boltzmann equation:

$$\frac{\partial f}{\partial t} + v\mu\frac{\partial f}{\partial x} = \frac{\langle f\rangle - f}{\tau} + Q \tag{2.1}$$

where

$$\langle f\rangle = \tfrac{1}{2}\int_{-1}^{1} f(x, t; v, \mu)\,\mathrm{d}\mu \qquad \mu = \cos\theta \tag{2.2}$$

subject to the initial condition

$$f(x, t; v, \mu) = A(x)B(\mu) \qquad \text{at time } t = 0. \tag{2.3}$$

In the following analysis, the particle speed is taken to be a constant parameter. In the above equations, $f(x, t; v, \mu)$ is the velocity space distribution function at position x and time t, for particles with speed v and pitch angle cosine $\mu = \cos\theta$; $\langle f\rangle$ is the mean distribution function averaged over μ, and $\tau = \tau(x, v)$ is the collision time. Fedorov and Shakhov (1993) and Fedorov *et al* (1995) obtained the Green function solution G of (2.1) with source term $Q = \delta(x - x_0)\delta(\mu - \mu_0)\delta(t)$, and with zero initial data ($A = B = 0$). Kota (1994) considered a similar solution of the Boltzmann equation (2.1) with an isotropic source term $Q = \delta(x - x_0)\delta(t)$ and also with zero inital data ($A = B = 0$). In this paper, we consider the solution of the initial value problem for (2.1) in which $f(x, 0; v, \mu) = \delta(x)\delta(\mu - \mu_0)$ and with zero source term $Q = 0$. This latter problem yields the same Green function obtained by Fedorov and Shakhov (1993) and Fedorov *et al* (1995). Thus, without loss of generality, we consider the case $Q \equiv 0$, and take $\tau = \tau(v)$ to be independent of x.

3. Integral equations and multiple scattering solutions

Formally integrating the characteristics for (2.1) with $Q = 0$, results in the integral equation:

$$f(x,t;v,\mu) = \int_0^t \langle f\rangle(x',t',v)\exp[-(t-t')/\tau]\,\mathrm{d}t' + f(x-v\mu t,0;v,\mu)\exp(-t/\tau) \quad (3.1)$$

where

$$x' = x - v\mu(t-t') \tag{3.2}$$

denotes the position of the particle at the last scatter. The second term on the right-hand side of (3.1) represents the unscattered particles and $P(t) = \exp(-t/\tau)$ is the probability that the initial particles have not been scattered at time t. Equation (3.1) is an integral equation for f in which $\langle f\rangle$ is given by (2.2). One can also average (3.1) over μ to obtain the integral equation

$$\langle f\rangle(x,t,v) = \tfrac{1}{2}\int_{-1}^{1}\mathrm{d}\mu\left(\int_0^t \langle f\rangle(x',t',v)\exp[-(t-t')/\tau]\,\mathrm{d}t' + f(x-v\mu t,0;v,\mu)\exp(-t/\tau)\right) \tag{3.3}$$

for $\langle f\rangle$. A similar integral equation formulation of the steady state BGK Boltzmann equation was used by Berezhko *et al* (1983) in a one-fluid, self-consistent model of cosmic ray modified shocks.

To develop a multiple scattering formalism for the BGK Boltzmann equation (2.1), with $Q = 0$, i.e.,

$$\frac{\mathrm{d}f}{\mathrm{d}t} = \frac{\langle f\rangle - f}{\tau} \qquad \frac{\mathrm{d}}{\mathrm{d}t} = \frac{\partial}{\partial t} + v\mu\frac{\partial}{\partial x} \tag{3.4}$$

we write the solution for f in the form

$$f = f_0 + f_c \qquad f_c = \sum_{n=1}^{\infty} f_n \tag{3.5}$$

where f_0 denotes the distribution of unscattered particles and f_n is the distribution of particles that have undergone n-scatters (e.g. Kuhn 1979). From physical reasons, the partial distribution functions $\{f_j : j = 0,1,2,\ldots\}$ satisfy the coupled evolution equations

$$\frac{\mathrm{d}f_0}{\mathrm{d}t} = -\frac{f_0}{\tau} \qquad \frac{\mathrm{d}f_n}{\mathrm{d}t} = \frac{\langle f_{n-1}\rangle}{\tau} - \frac{f_n}{\tau} \qquad n \geqslant 1. \tag{3.6}$$

In (3.6), the particles that have undergone $(n-1)$-scatters provide a source for the particles that will undergo n-scatters. The initial value data for (3.6) are

$$f_0 = A(x)B(\mu) \qquad f_n = 0 \qquad n \geqslant 1 \qquad \text{at time } t = 0 \tag{3.7}$$

since there are no scattered particles at time $t = 0$. The Neumann series of the Volterra-type integral equation (3.1) for f is obtained by using the iteration scheme

$$f^{(n)} = K[f^{(n-1)}] + f_0 \qquad f^{(0)} = f_0 \tag{3.8}$$

where $f^{(n)}$ is the nth iterate and K denotes the integral (and averaging) operator in (3.1). From (3.8),

$$f^{(N)} = (I + K + K^2 + \cdots + K^N)f_0 = f_0 + \sum_{n=1}^{N} f_n \tag{3.9}$$

where $f_n = K^n(f_0)$ is the distribution of particles that have undergone n-scatters. If the multiple scattering series (3.9) converges as $N \to \infty$ (which it does in this paper), letting $N \to \infty$ in (3.9) yields the required solution of the BGK Boltzmann equation in the form (3.5).

4. Solutions in Fourier–Laplace space

In order to solve the Boltzmann equation (3.4) and the multiple scattering equations (3.6) we introduce the Fourier and Laplace transforms:

$$\hat{f}(k, t; v, \mu) = \int_{-\infty}^{\infty} \frac{\mathrm{d}x}{2\pi} \exp(-\mathrm{i}kx) f(x, t; v, \mu) \tag{4.1}$$

$$\tilde{f}(k, s; v, \mu) = \int_{0}^{\infty} \mathrm{d}t \exp(-st) \hat{f}(k, t; v, \mu). \tag{4.2}$$

After determining the solution for $\tilde{f}$ in Laplace–Fourier space, the required solution for $f(x, t; v, \mu)$ is given by the standard inversion formula

$$f(x, t; v, \mu) = \frac{1}{2\pi\mathrm{i}} \int_{c-\mathrm{i}\infty}^{c+\mathrm{i}\infty} \mathrm{d}s \int_{-\infty}^{\infty} \mathrm{d}k \exp(st + \mathrm{i}kx) \tilde{f}(k, s; v, \mu) \tag{4.3}$$

where $\tilde{f}$ is required to be analytic on the inversion contour (for a discussion of the conditions under which the Fourier inversion theorem holds, and possible modifications of (4.3) to ensure convergence of the integrals, and the regions of analyticity of the transforms, see, for example, Morse and Feshbach (1953), volume 1).

Consider the initial value problem for (2.1)–(2.3) with $Q = 0$, where the particle speed v is a constant parameter. The solution can be written in the form

$$f(x, t; v, \mu) = \int_{-1}^{1} \mathrm{d}\mu_0\, B(\mu_0) \int_{-\infty}^{\infty} \mathrm{d}x_0\, A(x_0) G(\bar{x}, \bar{t}, v, \mu; \bar{x}_0, \mu_0) \tag{4.4}$$

where

$$\bar{x} = \frac{x}{v\tau} \qquad \bar{t} = \frac{t}{\tau} \tag{4.5}$$

are normalized space ($\bar{x}$) and time ($\bar{t}$) variables, respectively. The Green function G in (4.4) is the solution of the Boltzmann equation (3.4) satisfying the initial conditions

$$G(\bar{x}, 0, v, \mu; \bar{x}_0, \mu_0) = \delta(x - x_0)\delta(\mu - \mu_0). \tag{4.6}$$

Taking the Laplace and Fourier transforms of the Boltzmann equation (2.1) with zero source term, yields the equation

$$\tilde{G} - \frac{\langle \tilde{G} \rangle}{\nu + \mathrm{i}K\mu} = \frac{\tau \hat{G}(k, 0, v, \mu)}{\nu + \mathrm{i}K\mu} \equiv \frac{\tau \exp(-\mathrm{i}K\bar{x}_0)\delta(\mu - \mu_0)}{2\pi(\nu + \mathrm{i}K\mu)} \tag{4.7}$$

where

$$\nu = 1 + s\tau \qquad K = kv\tau \tag{4.8}$$

are dimensionless forms of s and k, and the angular brackets on $\langle \tilde{G} \rangle$ denote an average of $\tilde{G}$ over μ. Averaging (4.7) over μ yields the equation

$$\langle \tilde{G} \rangle [1 - a(K, \nu)] = \frac{\tau \exp(-\mathrm{i}K\bar{x}_0)}{4\pi(\nu + \mathrm{i}K\mu_0)} \tag{4.9}$$

for $\langle \tilde{G} \rangle$ where

$$a(K, \nu) = \left\langle \frac{1}{\nu + \mathrm{i}K\mu} \right\rangle = \frac{1}{2\mathrm{i}K} \ln\left(\frac{\nu + \mathrm{i}K}{\nu - \mathrm{i}K}\right). \tag{4.10}$$

From (4.7)–(4.10) it follows that the solution for $\tilde{G}$ in transform space can be written in the form

$$\tilde{G} = \tilde{G}_0 + \tilde{G}_c \tag{4.11}$$

where

$$\tilde{G}_0 = \frac{\tau \exp(-\mathrm{i}K\bar{x}_0)\delta(\mu - \mu_0)}{2\pi(\nu + \mathrm{i}K\mu)} \tag{4.12}$$

represents the unscattered particles and

$$\tilde{G}_c = \frac{\tau \exp(-\mathrm{i}K\bar{x}_0)}{4\pi[1 - a(K,\nu)](\nu + \mathrm{i}K\mu)(\nu + \mathrm{i}K\mu_0)} \tag{4.13}$$

represents the scattered particles.

Fedorov and Shakhov (1993) and Fedorov *et al* (1995) obtained the Green function G by first inverting the transforms (4.11)–(4.13) with respect to s and then with respect to k. Kota (1994) obtained a similar solution in which $f = \delta(x - x_0)$ at time $t = 0$ (more precisely, these authors solved the Boltzmann equation with non-zero source terms $Q = \delta(x-x_0)\delta(\mu-\mu_0)\delta(t)$ and $Q = \delta(x - x_0)\delta(t)$ respectively, in (2.1), with zero initial data; but these problems are equivalent to solving the homogeneous Boltzmann equation with singular initial conditions, which is the approach adopted in this work). The solutions obtained by Fedorov and Shakhov (1993) and Kota (1994) showed that the solution f_c for the scattered particles consisted of a superposition of slowly decaying diffusive-type modes, associated with the poles in the complex ν-plane that occur on the resonant manifold:

$$D(K,\nu) \equiv 1 - a(K,\nu) = 0 \tag{4.14}$$

plus fast decaying modes ($\propto \exp(-t/\tau)$) associated with the branch cut for $a(K,\nu)$ due to the logarithm in (4.10), as well as other fast decaying modes associated with the poles at $\nu = -\mathrm{i}K\mu$ and $-\mathrm{i}K\mu_0$. From (4.10) and (4.14), the diffusive modes satisfy the dispersion relation

$$\nu = K \cot K \qquad |K| < \tfrac{1}{2}\pi \tag{4.15}$$

where the restriction $|K| < \frac{1}{2}\pi$ is necessary if $a(K,\nu)$ is to be a single-valued function of ν for a fixed K.

It is straightforward to verify that the diffusive eigenmode

$$g = \frac{\exp[(\nu_a - 1)\bar{t} + \mathrm{i}K_a\bar{x}]}{\nu_a + \mathrm{i}K_a\mu} \qquad |K_a| < \tfrac{1}{2}\pi \tag{4.16}$$

where

$$\nu_a = K_a \cot K_a \tag{4.17}$$

satisfies the BGK Boltzmann equation (2.1) with $Q = 0$ (see also Kota 1994). It is of interest to note that the Fourier–Laplace transform of g:

$$\tilde{g} = \frac{\nu\tau^2\delta(K - K_a)}{(\nu - \nu_a)(\nu_a + \mathrm{i}K_a\mu)} \tag{4.18}$$

is singular on the resonant manifold (4.14). One can verify that $\tilde{g}$ satisfies Fourier space equations analogous to (4.7)–(4.9).

4.1. Multiple scattering approach

One can also solve (3.6) for the partial distributions f_n of particles that have undergone n-scatters. In Fourier–Laplace space (3.6) reduce to

$$\tilde{G}_n = \frac{\langle \tilde{G}_{n-1}\rangle}{\nu + \mathrm{i}K\mu} \qquad n \geqslant 1 \tag{4.19}$$

for the scattered distributions, where we restrict our attention to the Green function case. The unscattered particles $\tilde{G}_0$ are given by (4.12). Averaging (4.19) over μ yields the recurrence relations

$$\langle \tilde{G}_n \rangle = a \langle \tilde{G}_{n-1} \rangle \qquad n \geqslant 1 \tag{4.20}$$

for the mean distributions $\langle \tilde{G}_n \rangle$, where $a(K, \nu)$ is given by (4.10). From (4.20)

$$\langle \tilde{G}_n \rangle = a^n \langle \tilde{G}_0 \rangle \equiv \frac{\tau a^n \exp(-\mathrm{i} K \bar{x}_0)}{4\pi(\nu + \mathrm{i} K \mu_0)}. \tag{4.21}$$

Using (4.21) in (4.19) yields the formula

$$\tilde{G}_n = \frac{\tau a^{n-1} \exp(-\mathrm{i} K \bar{x}_0)}{4\pi(\nu + \mathrm{i} K \mu)(\nu + \mathrm{i} K \mu_0)} \tag{4.22}$$

for the distribution of particles that have done n-scatters ($n \geqslant 1$).

By summing the partial distributions $\tilde{G}_n$ we obtain

$$\tilde{G}_c = \sum_{n=1}^{\infty} \tilde{G}_n = \left(\sum_{n=1}^{\infty} a^{n-1} \right) \frac{\langle \tilde{G}_0 \rangle}{\nu + \mathrm{i} K \mu} = \frac{\langle \tilde{G}_0 \rangle}{(1 - a)(\nu + \mathrm{i} K \mu)} \tag{4.23}$$

which is equivalent to (4.13) for $\tilde{G}_c$. In order that the geometric series in (4.23) converge, it is necessary that $|a(K, \nu)| < 1$ on the integration path used in the inversion (4.3).

The above analysis shows that the complicated integral and averaging operator occurring in the integral equation formulation (3.3) corresponds to multiplication by $a(K, \nu)$ in Fourier–Laplace space. In the next section the partial distributions $\{G_n : n \geqslant 0\}$ are obtained by Fourier–Laplace inversion. By summing the multiple scattering series, we also obtain the Green function solution form obtained by Fedorov and Shakhov (1993) and Fedorov *et al* (1995). It is of interest to note that the diffusive eigenmodes (4.16), which dominate the solution for G_c at late times, can be decomposed into a multiple scattering series, in which each term is a fast decaying mode.

5. Green function solutions

In this section, the Green function solution G of the BGK Boltzmann equation is determined by inverting the solution for $\tilde{G}$ in Fourier–Laplace space obtained in section 4. In section 5.1, explicit formulae are obtained for the distribution of unscattered particles G_0; the distribution of particles that have undergone n-scatters $\{G_n : n \geqslant 1\}$; and the total scattered distribution G_c, where

$$G = G_0 + G_c \qquad G_c = \sum_{n=1}^{\infty} G_n. \tag{5.1}$$

In section 5.2, the Fedorov–Shakhov form of the Green function G is obtained by summing the multiple scattering series for G_c. The detailed demonstration that the multiple scattering series, and the Fedorov–Shakhov solution form are equivalent involves contour integration, the details of which are described in appendix B.

5.1. The multiple scattering series

Either by inverting (4.12) (appendix A), or by using the integral equation formulation (3.1), we find

$$G_0 = \exp(-t/\tau)\delta(x - x_0 - v\mu t)\delta(\mu - \mu_0) \tag{5.2}$$

is the Green function solution for the unscattered particles.

Using the Laplace–Fourier inversion formula (4.3), in conjunction with the expressions (4.22) for the $\{\tilde{G}_n\}$, yields the distribution of particles G_n that have done n-scatters, in the form:

$$G_n = \frac{\exp(-\bar{t})}{2v\tau(\mu-\mu_0)}\Bigg[-\frac{1}{\pi}\int_{-1}^{1}\left(\frac{1}{p-\mu}-\frac{1}{p-\mu_0}\right)V_n^-(y,\bar{t},p) \\ \times[H(y)H(p)-H(-y)H(-p)]\,\mathrm{d}p \\ +V_n^+(y,\bar{t},\mu)[H(y)H(\mu)-H(-y)H(-\mu)] \\ -V_n^+(y,\bar{t},\mu_0)[H(y)H(\mu_0)-H(-y)H(-\mu_0)]\Bigg] \tag{5.3}$$

($n \geqslant 1$), where

$$y = \bar{x}-\bar{x}_0. \tag{5.4}$$

The functions $V_n^{\pm}(y,\bar{t},p)$ in (5.3) are defined by the equations

$$V_n^{\pm}(y,\bar{t},p) = \hat{V}_n^{\pm}(y,\bar{t},p)H\left(\bar{t}-\frac{y}{p}\right) \tag{5.5}$$

$$\hat{V}_n^{-}(y,\bar{t},p) = \mathrm{Im}\,([m(p)+\mathrm{i}\pi]^{n-1})\frac{[\frac{1}{2}(y-p\bar{t})]^{n-1}}{(n-1)!} \tag{5.6}$$

$$\hat{V}_n^{+}(y,\bar{t},p) = \mathrm{Re}\,([m(p)+\mathrm{i}\pi]^{n-1})\frac{[\frac{1}{2}(y-p\bar{t})]^{n-1}}{(n-1)!} \tag{5.7}$$

where

$$m(p) = \ln\left(\frac{1-p}{1+p}\right) \qquad \text{and} \qquad |p|<1. \tag{5.8}$$

In the above equations $H(x)$ denotes the Heaviside step function. The integral in (5.3) is a Cauchy principal (CPV) integral, with singularities at $p=\mu$ and μ_0, and Re (z) and Im (z) denote the real and imaginary parts of the complex number z. The functions $V_n^{\pm}(y,\bar{t},p)$ are only non-zero for $|p|\bar{t} > |\bar{x}-\bar{x}_0|$, which corresponds to the causality constraint due to the finite particle speed v, which implies $|(\bar{x}-\bar{x}_0)/\bar{t}| < |p| < 1$ in the CPV integral. A sketch of the derivation of (5.3)–(5.8) is given in appendix A.

In the next section the Fedorov and Shakhov (1993) and Fedorov *et al* (1995) form of the Green function G_c is obtained from the multiple scattering series (5.1).

5.2. The Fedorov–Shakhov solution form

By inverting the transform (4.13) (first with respect to ν and then with respect to K), Fedorov and Shakhov (1993) obtained the Green function G_c for the scattered particles in the form

$$G_c = \frac{\exp(-\bar{t})}{2\pi v\tau}\int_{-1}^{1}\frac{\mathrm{d}p}{(p-\mu)(p-\mu_0)}\sin\left[\frac{1}{2}\pi(y-p\bar{t})\right]\Gamma(y,\bar{t},p) \\ +\frac{\exp(-\bar{t})}{2v\tau(\mu-\mu_0)}\left(\Gamma(y,\bar{t},\mu_0)\cos\left[\frac{1}{2}\pi(y-\mu_0\bar{t})\right]\right. \\ \left.-\Gamma(y,\bar{t},\mu)\cos\left[\frac{1}{2}\pi(y-\mu\bar{t})\right]\right)+\frac{1}{2\pi v\tau}\int_0^{\frac{\pi}{2}}\mathrm{d}K\exp[(K\cot K-1)\bar{t}] \\ \times\frac{\cos(Ky)[\cos^2K-\mu\mu_0\sin^2K]+\sin(Ky)\sin K\cos K(\mu+\mu_0)}{(\cos^2K+\mu_0^2\sin^2K)(\cos^2K+\mu^2\sin^2K)} \tag{5.9}$$

where

$$\Gamma(y, \bar{t}, p) = \left|\frac{1-p}{1+p}\right|^{\frac{1}{2}(y-p\bar{t})} [H(y-p\bar{t})H(p) - H(p\bar{t}-y)H(-p)]. \quad (5.10)$$

The last term on the right-hand side of (5.9) (the integral from $K = 0$ to $\frac{1}{2}\pi$) consists of a superposition of slowly decaying diffusive eigenmodes of the form (4.16) (see appendix B), whereas the remaining terms on the right-hand side of (5.9) consist of fast decaying modes. The main purpose of this section is to show how the Fedorov–Shakhov solution (5.9) arises from summing the multiple scattering series (5.1).

To derive the solution (5.9) from the multiple scattering series, first note from (5.1) and (5.3) that

$$G_c = G_c^{(\mathrm{CPV})} + G_c^{(\mu\mu_0)} \quad (5.11)$$

where

$$G_c^{(\mathrm{CPV})} = \sum_{n=1}^{\infty} G_n^{(\mathrm{CPV})} \qquad G_c^{(\mu\mu_0)} = \sum_{n=1}^{\infty} G_n^{(\mu\mu_0)}. \quad (5.12)$$

In (5.12) the superscripts (CPV) and $(\mu\mu_0)$ refer to the CPV integral and non-CPV contributions to the G_n in (5.3).

By using the identity

$$H[\bar{t} - y/p] \equiv H(p)[1 - H(y-p\bar{t})] + H(-p)[1 - H(p\bar{t}-y)] \quad (5.13)$$

for the Heaviside step function $H(x)$, the CPV sum in (5.12) may be written in the form

$$\begin{aligned} G_c^{(\mathrm{CPV})} = {} & \frac{\exp(-\bar{t})}{2\pi v\tau} \fint_{-1}^{1} \frac{\mathrm{d}p}{(p-\mu)(p-\mu_0)} \sin\left[\frac{1}{2}\pi(y-p\bar{t})\right] \Gamma(y, \bar{t}, p) \\ & - \frac{\exp(-\bar{t})}{2\pi v\tau} \sum_{n=1}^{\infty} \fint_{-1}^{1} \frac{\mathrm{d}p}{(p-\mu)(p-\mu_0)} \hat{V}_n^{-}(y, \bar{t}, p) \\ & \times [H(y)H(p) - H(-y)H(-p)]. \end{aligned} \quad (5.14)$$

The first CPV integral on the right-hand side of (5.14) involving $\Gamma(y, \bar{t}, p)$ is part of the Fedorov–Shakhov solution form (5.9).

Similarly, using the identity (5.13) in (5.3), we obtain

$$\begin{aligned} G_c^{(\mu\mu_0)} = {} & \frac{\exp(-\bar{t})}{2v\tau(\mu-\mu_0)} \left(\Gamma(y, \bar{t}, \mu_0) \cos\left[\frac{1}{2}\pi(y-\mu_0\bar{t})\right] - \Gamma(y, \bar{t}, \mu) \cos\left[\frac{1}{2}\pi(y-\mu\bar{t})\right]\right) \\ & + \frac{\exp(-\bar{t})}{2v\tau(\mu-\mu_0)} (\hat{V}^{+}(y, \bar{t}, \mu)[H(y)H(\mu) - H(-y)H(-\mu)] \\ & - \hat{V}^{+}(y, \bar{t}, \mu_0)[H(y)H(\mu_0) - H(-y)H(-\mu_0)]) \end{aligned} \quad (5.15)$$

for the non-CPV integral contribution to G_c, where

$$\hat{V}^{+}(y, \bar{t}, \mu) = \left|\frac{1-\mu}{1+\mu}\right|^{\frac{1}{2}(y-\mu\bar{t})} \cos\left[\frac{1}{2}\pi(y-\mu\bar{t})\right]. \quad (5.16)$$

The terms involving Γ are readily recognized as part of the Fedorov–Shakhov solution form (5.9).

Adding the CPV contribution (5.14) for G_c to the non-CPV term $G_c^{(\mu\mu_0)}$ in (5.15) and using the identity (see appendix B)

$$-\frac{\exp(-\bar{t})}{2\pi v\tau} \sum_{n=1}^{\infty} \fint_{-1}^{1} \frac{\mathrm{d}p}{(p-\mu)(p-\mu_0)} \hat{V}_n^{-}(y, \bar{t}, p)[H(y)H(p) - H(-y)H(-p)]$$

$$
\begin{aligned}
&+\frac{\exp(-\bar{t})}{2v\tau(\mu-\mu_0)}(\hat{V}^{+}(y,\bar{t},\mu)[H(y)H(\mu)-H(-y)H(-\mu)]\\
&-\hat{V}^{+}(y,\bar{t},\mu_0)[H(y)H(\mu_0)-H(-y)H(-\mu_0)])\\
&=\frac{1}{2\pi v\tau}\int_0^{\frac{\pi}{2}}\mathrm{d}K\exp[(K\cot K-1)\bar{t}]\\
&\times\frac{\cos(Ky)[\cos^2K-\mu\mu_0\sin^2K]+\sin(Ky)\sin K\cos K(\mu+\mu_0)}{(\cos^2K+\mu_0^2\sin^2K)(\cos^2K+\mu^2\sin^2K)}
\end{aligned}
\tag{5.17}
$$

yields the solution (5.9) for G_c obtained by Fedorov and Shakhov (1993).

The solution (5.9) obtained by Fedorov and Shakhov (1993) consists of a sum of non-causal terms, namely the diffusive eigenmodes contribution (the integral from $K=0$ to $\frac{1}{2}\pi$), and the remaining terms involving $\Gamma(y,\bar{t},p)$. Most of the separate terms in (5.9) are non-zero for $|\bar{x}-\bar{x}_0|>\bar{t}$. However, the total expression for G_c clearly satisfies the causality constraint that $G_c=0$ for $|\bar{x}-\bar{x}_0|>\bar{t}$, since it is equivalent to summing the multiple scattering series (note that each term in the multiple scattering series is zero for $|\bar{x}-\bar{x}_0|>\bar{t}$).

5.3. Alternative form for G_n

The Fedorov–Shakhov solution (5.9) for the total scattered particle Green function G_c, consists of a superposition of fast decaying modes, plus more slowly decaying diffusive eigenmodes (the integral from $K=0$ to $\frac{1}{2}\pi$ in (5.9)). This suggests that the Green function G_n for particles that have done n-scatters can be rewritten in a form that emphasizes the diffusive eigenmodes. Using (B.9)–(B.12) and the results of section 5.2, the Green function G_n in (5.3) can be written in the form

$$
\begin{aligned}
G_n=I_{n-1}+\frac{\exp(-\bar{t})}{2v\tau(\mu-\mu_0)}\Bigg[&\frac{1}{\pi}\int_{-1}^{1}\mathrm{d}p\left(\frac{1}{p-\mu}-\frac{1}{p-\mu_0}\right)\\
&\times\hat{V}_n^{-}(y,\bar{t},p)[H(y-p\bar{t})H(p)-H(p\bar{t}-y)H(-p)]\\
&+\hat{V}_n^{+}(y,\bar{t},\mu_0)[H(y-\mu_0\bar{t})H(\mu_0)-H(\mu_0\bar{t}-y)H(-\mu_0)]\\
&-\hat{V}_n^{+}(y,\bar{t},\mu)[H(y-\mu\bar{t})H(\mu)-H(\mu\bar{t}-y)H(-\mu)]\Bigg]
\end{aligned}
\tag{5.18}
$$

where $y=\bar{x}-\bar{x}_0$, and

$$
I_{n-1}=\frac{\exp(-\bar{t})}{2\pi v\tau}\frac{1}{(n-1)!}\int_0^{\frac{\pi}{2}}\mathrm{d}K\,\mathrm{Re}\left(\frac{(\mathrm{i}Ky+K\cot K\bar{t})^{n-1}}{(\cos K+\mathrm{i}\mu\sin K)(\cos K+\mathrm{i}\mu_0\sin K)}\right)
\tag{5.19}
$$

(see appendix B). The alternative form for I_{n-1} in (B.11) corresponds to the solution form (5.3) for G_n.

The integral I_{n-1} in (5.18) and (5.19) dominates the late-time behaviour of G_n. In fact, $G_d=\sum_{n=1}^{\infty}I_{n-1}$ gives the diffusive eigenmode contribution to G_c in the Fedorov–Shakhov solution (5.9) (the integral from $K=0$ to $\frac{1}{2}\pi$ in (5.9); see also appendix B). Thus, (5.18) and (5.19) provide an alternative representation of G_n to that in (5.3) which emphasizes the late-time behaviour and the diffusive eigenmodes.

6. Numerical examples

Figure 1 shows some of the main features of the Fedorov–Shakhov solution (5.9) and (5.10) for the Green function G_c of scattered particles. The figure shows the variation of G_c as a function of $\bar{t}$ for a range of pitch angle cosines μ ($\mu=-0.98, 0.001, 0.49$ and 0.98) at position

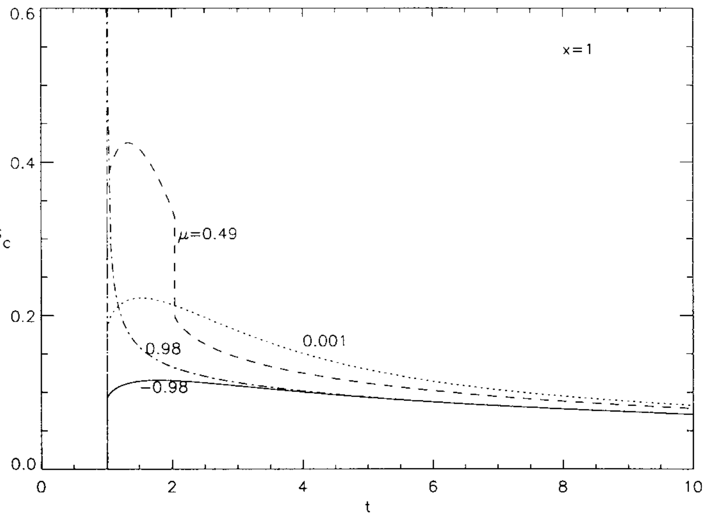

Figure 1. The scattered Green function G_c of (5.9) versus normalized time $\bar{t}$. The parameters used are $\bar{x}_0 = 0$, $\bar{x} = 1$, $\mu_0 = 0.99$, and the different curves are for $\mu = -0.98$, 0.001, 0.49 and 0.98.

$\bar{x} = 1$, for particles initially located at $\bar{x}_0 = 0$ with $\mu = \mu_0 = 0.99$ at time $t = 0$ (Fedorov and Shakhov (1993) and Fedorov *et al* (1995) show similar figures). The main points to note are the strongly anisotropic character of the distribution at early times ($1 < \bar{t} < 2$ say), and the near isotropy of the distributions at late times ($\bar{t} \sim 10$). This is intuitively expected since at early times, the particles will have undergone only a few scatters, and consequently are still highly beamed about the initial particle direction with $\mu = \mu_0 = 0.99$, whereas at late times the particles are isotropized by many scatters.

Figure 2 shows further examples of the Fedorov–Shakhov solution for G_c at $x = 0.001$ and at $x = -1$, for the same values of μ and μ_0 as in figure 1 ($x_0 = 0$, $\mu_0 = 0.99$; $\mu = -0.98$, 0.001, 0.49, and 0.98). In figure 2(*a*) ($x = 0.001$), the distribution for G_c for $\mu = 0.001$ has discontinuities at $\bar{t} = \bar{x}/\mu = 1$, and at $\bar{t} = \bar{x}/\mu_0 = 1.0101 \times 10^{-3}$, which is similar to the the curve $\mu = 0.49$ in figure 1, where $\bar{x} = 1$. These discontinuities are due to particles that have undergone a single scatter (i.e. G_1). The curve for G_c for $\mu = 0.001$ in the top panel exhibits two maxima: one near $\bar{t} = \bar{x}/\mu_0 = 1.0101 \times 10^{-3}$, due to particles that have experienced a single scatter, and one at $\bar{t} \simeq 2.5$ due to particles that have undergone multiple scatters. Figure 2(*b*) ($\bar{x} = -1$) indicates that at early times, the almost backward propagating particles with $\mu = -0.98$, dominate the distribution G_c. The peak in the distribution for $\mu = -0.98$, is presumably due to particles initially moving in the forward direction with $\mu \simeq \mu_0 = 0.99$ which have undergone a single scatter.

Figure 3 shows again the curve $\mu = 0.49$ for G_c in figure 1, and the distributions $\{G_n : 1 \leqslant n \leqslant 10\}$ of particles that have done n-scatters, as functions of $\bar{t}$. Also shown for comparison is the approximate solution

$$S_N = \sum_{n=1}^{N} G_n \tag{6.1}$$

obtained by summing the multiple scattering series. In the example in figure 3, the approximate solution S_{10} is shown by the dotted curve. As in figure 1, $\bar{x}_0 = 0$, $\bar{x} = 1$, and $\mu_0 = 0.99$. The distributions were evaluated numerically using the solution form (5.18) and (5.19). Note that both $G_c = 0$ and $G_n = 0$ for $\bar{t} < |\bar{x}|$ due to the causality constraint that the particle cannot

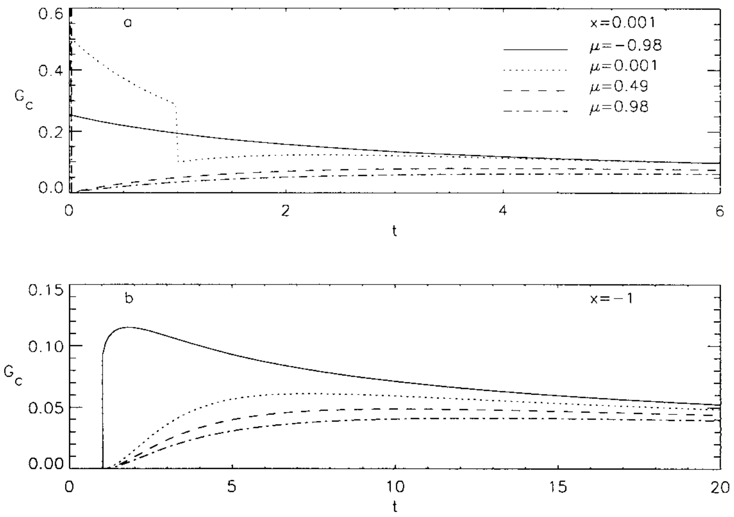

Figure 2. The Green function G_c of (5.9) versus $\bar{t}$. The parameters are the same as in figure 1, except that $\bar{x} = 0.001$ in (*a*) and $\bar{x} = -1$ in (*b*). As in figure 1, $\mu_0 = 0.99$, $\bar{x}_0 = 0$ and $\mu = -0.98$, 0.001, 0.49 and 0.98.

travel a distance $\Delta x > vt$ in time t. At early times the solution for G_c and the approximation S_N in figure 3, are dominated by the Green G_1 representing particles that have undergone a single scatter. From (5.3)–(5.7), G_1 is given by

$$G_1 = \frac{\exp(-\bar{t})}{2v\tau(\mu - \mu_0)} \left[H\left(\bar{t} - \frac{y}{\mu}\right)[H(y)H(\mu) - H(-y)H(-\mu)] \right.$$
$$\left. -H\left(\bar{t} - \frac{y}{\mu_0}\right)[H(y)H(\mu_0) - H(-y)H(-\mu_0)] \right] \tag{6.2}$$

where $y = \bar{x} - \bar{x}_0$. For the example in figure 3, G_1 is only non-zero for $\bar{t}$ in the range

$$1 < \frac{\bar{x}}{\mu_0} < \bar{t} < \frac{\bar{x}}{\mu}. \tag{6.3}$$

In this case, G_1 may be written in the simpler form

$$G_1 = \frac{\exp(-\bar{t})}{2v\tau(\mu - \mu_0)} \left[H\left(\bar{t} - \frac{\bar{x}}{\mu}\right) - H\left(\bar{t} - \frac{\bar{x}}{\mu_0}\right) \right]. \tag{6.4}$$

Thus, the solution for G_1 consists of an exponentially damped profile in $\bar{t}$, with cut-offs in $\bar{t}$ at $\bar{t} = \bar{x}/\mu_0$ and at $\bar{t} = \bar{x}/\mu$. In the limit as $\mu \to \mu_0$ in (6.4),

$$G_1 \to \frac{\bar{x}\exp(-\bar{t})}{2v\tau\mu_0^2} \delta\left(\bar{t} - \frac{\bar{x}}{\mu_0}\right) \tag{6.5}$$

so that G_1 is singular as $\mu \to \mu_0$. There is no CPV integral contribution to G_1 in (5.3), or (6.2), because $\hat{V}_1^- = 0$ and $\hat{V}_1^+ = 1$ in (5.3).

At late times $\bar{t} \gg |\bar{x} - \bar{x}_0|$, the solution for G_c is roughly approximated by the diffusion equation Green function, i.e.,

$$G_c \simeq \frac{1}{4(\pi\kappa t)^{\frac{1}{2}}} \exp\left(-\frac{(x - x_0)^2}{4\kappa t}\right) \tag{6.6}$$

where $\kappa = v^2\tau/3$ is the diffusion coefficient (see, for example, appendix C). In figure 3, $G_c \simeq 0.1$ at $\bar{t} = 6$, whereas the diffusion approximation (6.6) yields $G_c \sim 0.08$. The

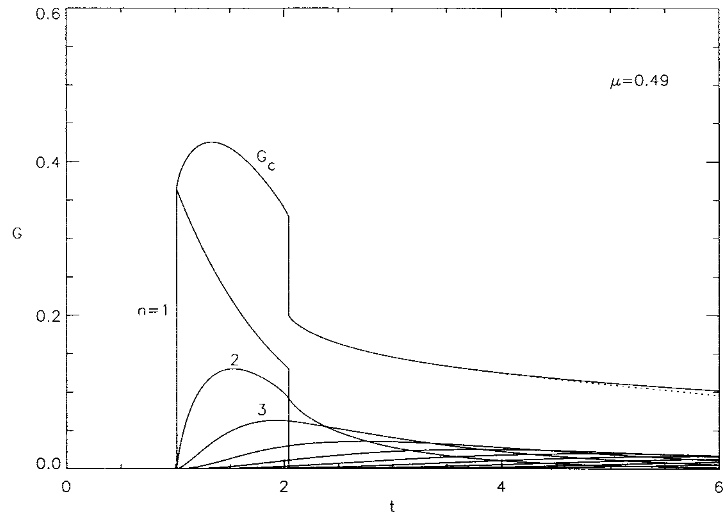

Figure 3. The plot shows G_c and $\{G_n : 1 \leqslant n \leqslant 10\}$ of particles that have done n-scatters, and the approximation S_{10} of particles that have done $N = 10$ scatters (the dotted curve). The parameters are $\bar{x} = 1$, $\bar{x}_0 = 0$, $\mu_0 = 0.99$ and $\mu = 0.49$ (this corresponds to the curve $\mu = 0.49$ in figure 1).

results in figure 3 indicate that the sum of the first ten terms of the multiple scattering series yields a reasonable approximation for G_c for $1 < \bar{t} < 6$, and $\bar{x} = 1$. However, as $\bar{t}$ increases, substantially more terms in the multiple scattering series are required for a good approximation to G_c. Other approximate solutions based on Legendre polynomial or eigenfunction expansions (e.g. Earl 1974, Weinberg and Wigner 1958), and perturbation methods using both eigenfunction expansions and scale analysis (e.g. Gombosi *et al* 1993) are useful in obtaining diffusion equation or telegraph equation approximations. Kota (1994) discusses the telegraph equation result of Gombosi *et al* (1993) by expanding the diffusive eigenmode dispersion equation (4.15) for small s and K (see also appendix C). A recent exposition of Legendre polynomial expansion solution techniques for the BGK Boltzmann equation that can deal with both anisotropic solutions at early times, and nearly isotropic distributions at late times has been developed by Zank *et al* (1999).

Figure 4 shows further examples of the decomposition of the solutions for G_c into its multiple scattering components G_n. The parameters are the same as in figure 1 (i.e. $\bar{x}_0 = 0$, $\bar{x} = 1$, $\mu_0 = 0.99$; the different panels are for $\mu = -0.98$, 0.001, 0.49 and 0.98). The dotted curves correspond to the multiple scattering series approximation (6.1) with $N = 10$ terms, which is a good approximation to G_c for $1 < \bar{t} < 6$. At early times, the distributions for G_c are anisotropic, and are in general of larger amplitude in the forward direction (figures 4(c) and (d)) than in the transverse (figure 4(b)) and backward direction (figure 4(a)). For $\mu = 0.98$ (figure 4(d)), the distribution G_1 is a very narrow, large amplitude pulse (from (6.3), the maximum height of the pulse is $G_c = 18.21$ at time $\bar{t} = \bar{x}/\mu_0 = 1.0101$, and $G_1 \neq 0$ for $1.0101 < \bar{t} < 1.0204$). From (6.2),

$$G_1 = \frac{\exp(-\bar{t})}{2v\tau(\mu_0 - \mu)} H\left(\bar{t} - \frac{\bar{x}}{\mu_0}\right) \tag{6.7}$$

for $\mu < 0$, $\mu_0 > 0$, $\bar{x}_0 = 0$ and $\bar{x} > 0$. Thus, G_1 has no upper cut-off in $\bar{t}$ in figure 4(a). Again note that G_c is nearly isotropic at the larger values of $\bar{t}$ ($G_c \sim 0.1$ at $\bar{t} = 6$), as expected from the diffusion equation approximation (6.6).

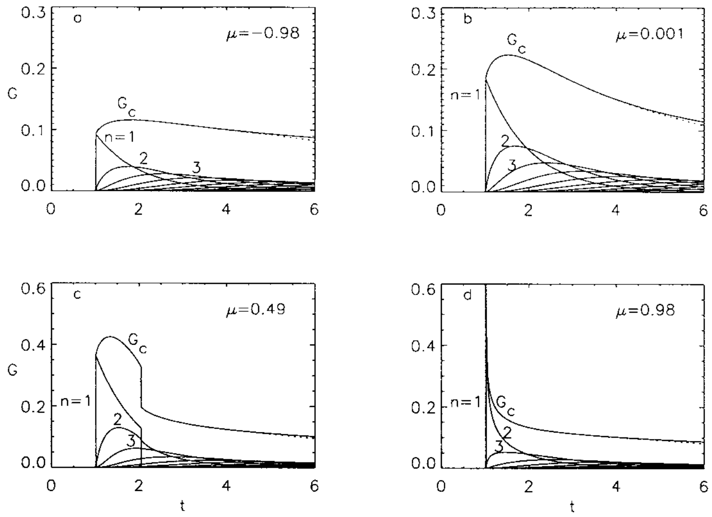

Figure 4. The plot shows examples of G_c and $\{G_n : 1 \leqslant n \leqslant 10\}$ versus $\bar{t}$. The dotted curves show the approximations S_{10} of particles that have done at most $N = 10$ scatters (the dotted curves). The parameters are the same as in figure 1 ($\bar{x}_0 = 0$, $\bar{x} = 1$, $\mu_0 = 0.99$, and the different plots ((*a*)–(*d*)) are for $\mu = -0.98$, 0.001, 0.49 and 0.98).

Although the use of $N = 10$ terms in the series (6.1) suffices for $1 < \bar{t} < 6$ in figures 3 and 4, a larger number of terms is needed to obtain an accurate solution for larger $\bar{t}$. This is illustrated in figure 5, which shows the Fedorov–Shakhov solution G_c, the distributions $\{G_n : 1 \leqslant n \leqslant 10\}$, and the approximation S_{10} (the dotted curve) for case $\mu = 0.001$ of figure 4, with $1 < \bar{t} < 20$. Clearly, more terms are needed in the multiple scattering series for $\bar{t} > 7$. Figure 6 shows the improvement over the approximation S_N used in figure 5 obtained by using successively larger values of N ($N = 10$, 15, 20, 25). The curve corresponding to $N = 30$ (unlabelled), is almost indistinguishable from the full solution for G_c for $1 < \bar{t} < 20$.

Figures 7 and 8 show further examples of the convergence of the multiple scattering series for $\mu = 0.49$, $\mu_0 = 0.99$ and $\bar{x} = -1$ (compare with the bottom panel of figure 2). Figure 7 shows the total scattered distribution G_c; the distributions $\{G_n : 1 \leqslant n \leqslant 10\}$ and the approximation S_{10} (the dotted curve). Note that in figure 7, $G_1 = 0$, and the scattered particles have done $n \geqslant 2$ scatters. This is intuitively expected, since the original particles with $\mu = \mu_0 > 0$, must scatter into the $\mu < 0$ hemisphere to reach $x = -1$, and hence particles with $\mu > 0$ at $x = -1$ must have done at least two scatters. The approximation S_{10} in figure 7 is a reasonable approximation for $1 < \bar{t} < 5$, but the approximation quickly degenerates in accuracy with increasing $\bar{t} > 5$. Figure 8 shows the improvement of the approximation S_N (the dotted curves) as N increases ($N = 10$, 15, 20, 25 and 30).

7. Summary and concluding remarks

In this paper, we have provided a multiple scattering formulation for the BGK Boltzmannn equation. The main aim of the paper was to provide the distributions of particles that have done n-scatters for the Green function solution investigated by Fedorov and Shakhov (1993) and Fedorov *et al* (1995). This information is not accessible in the solution form given by the above authors.

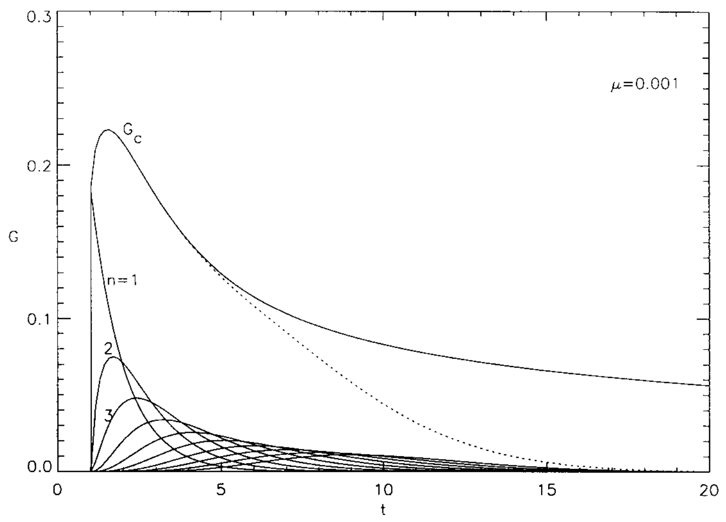

Figure 5. The plot shows G_c and $\{G_n : 1 \leqslant n \leqslant 10\}$, and the approximation S_{10} of particles that have done at most $N = 10$ scatters (the dotted curve) as functions of $\bar{t}$ for the case $\mu = 0.001$. The other parameters are the same as in figure 1 ($\bar{x} = 1$, $\bar{x}_0 = 0$, $\mu_0 = 0.99$). Note that S_{10} is a good approximation for $1 \leqslant \bar{t} \leqslant 5$, but a poor approximation for much larger $\bar{t}$.

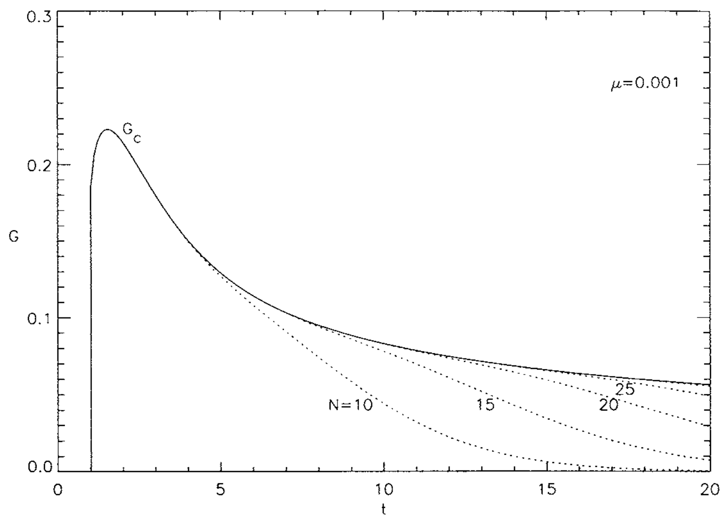

Figure 6. The plot shows how the multiple scattering series approximation S_N of (6.1) (the dotted curves) improves with increasing N ($N = 10, 15, 20, 25, 30$). The pitch angle cosine $\mu = 0.001$ and the other parameters are the same as in figure 1.

In the multiple scattering method, the distribution function $f = f_0 + f_c$ is split up into scattered (f_c) and unscattered (f_0) particles. The scattered distribution $f_c = \sum_{n=1}^{\infty} f_n$ is split up into particles that have done n-scatters $\{f_n\}$, where $n = 1, 2 \ldots$. Thus, the multiple scattering series provides statistical details of the complete solution for f, that are not readily apparent using other methods (one could, of course, obtain similar information by using Monte Carlo methods, in which the path of individual particles is monitored).

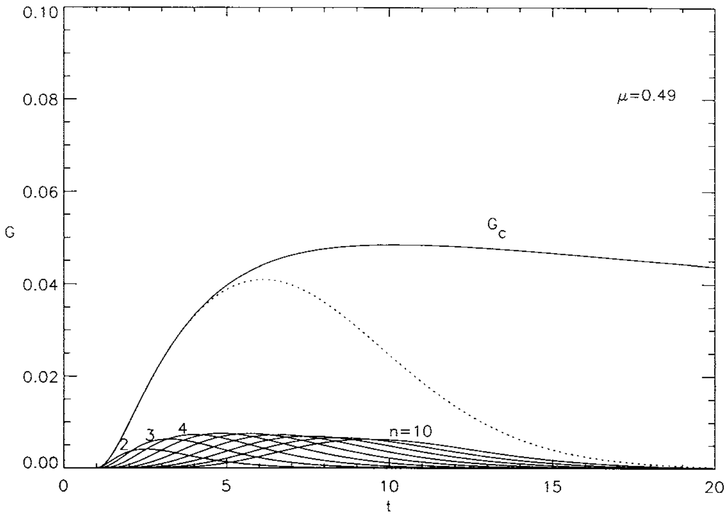

Figure 7. The same as figure 5, except that $\bar{x} = -1$ and $\mu = 0.49$.

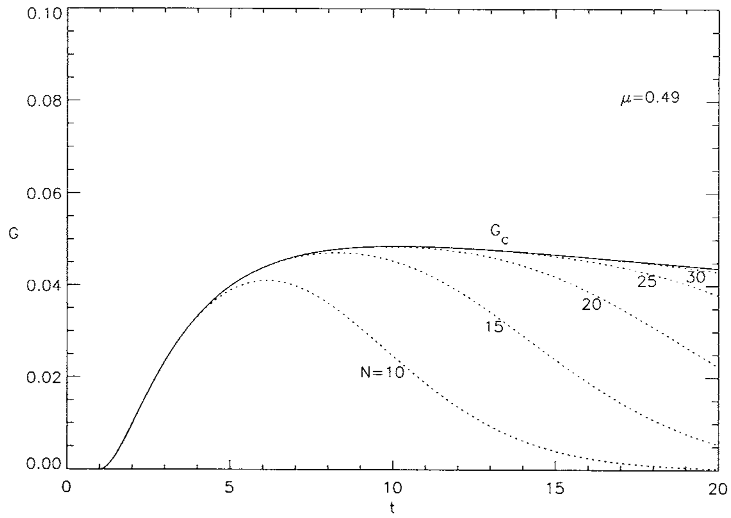

Figure 8. The same as figure 6, except that $\bar{x} = -1$ and $\mu = 0.49$.

In the multiple scattering approach, the unscattered particles f_0 provide a source for the particles f_1 that undergo a single scatter, and consequently, the unscattered particles decay exponentially as $f_0 \propto \exp(-t/\tau)$. The evolution equation for particles that have done n-scatters has the same form as the usual Boltzmann equation, except that the particles scattered into a given phase-space volume element consist of the particles that have done $(n-1)$-scatters (f_{n-1}), whereas the particles scattered out of the same phase-space volume element are particles of the nth scattered generation (f_n). This leads to an infinite coupled set of Boltzmann-like evolution equations (3.6). This system of equations may be solved sequentially proceeding from the $n = 0$ equation for the unscattered particles, and then proceeding to solve for the higher-order scattered distributions.

By integrating along the characteristics, the Boltzmann equation (2.1) may be cast in the form of an integral equation (3.1), in which f is given as an integral over $\langle f \rangle$ at the last scatter, multiplied by the probability that the particle remain unscattered in travelling from the position of the last scatter to its present position, plus an exponentially decaying distribution of the initial unscattered particles. The Neumann series obtained by iteration of this integral equation yields the multiple scattering series, in which the Nth iterate $S_N = \sum_{n=0}^{N} f_n$, yields the approximate solution of the Boltzmann equation consisting of particles that have done at most N-scatters. By letting $N \to \infty$, in the sequence of partial sums S_N, yields the complete solution for f in the form: $f = \lim_{N\to\infty} S_N = f_0 + f_c$.

The multiple scattering equations for the Green functions $\{G_n\}$ of particles that have done n-scatters were first solved by using Fourier and Laplace transforms to obtain the required solutions $\{\tilde{G}_n\}$ in transform space. The solutions in (x, t)-space were then obtained by Fourier–Laplace inversion (section 5). The solutions for the $\{\tilde{G}_n\}$ in transform space form a geometric progression: $\tilde{G}_n = a(K, \nu)\tilde{G}_{n-1}$, with common ratio $a(K, \nu)$ (K and $\nu = 1 + s\tau$ are the Fourier and Laplace transform variables), and the solution $\tilde{G}_c$ for the total scattered Green function depends on the singular resonant manifold $D(K, \nu) = 1 - a(K, \nu) = 0$, associated with slowly decaying diffusive eigenmodes in (x, t)-space (see also Kota 1994). The total scattered Green function $\tilde{G}_c = \sum_{n=1}^{\infty} \tilde{G}_n$ may also be obtained by use of the usual formula for the sum of a geometric progression.

The Green function G_n in (x, t)-space can be expressed in two different forms: the first form (5.3) shows that $G_n \neq 0$ for $|x - x_0| < vt$ and $G_n = 0$ for $|x - x_0| > vt$, which corresponds to the causality constraint that particles with speed v travel at most a distance $|x - x_0| = vt$ in time t. The second form of G_n in (5.18) emphasizes the diffusive behaviour of G_n at late times t. This second form of G_n is directly related to the form of the total scattered Green function G_c (5.9) obtained by Fedorov and Shakhov (1993) and Fedorov *et al* (1995), which also emphasizes the diffusive character of G_c at late times. The Fedorov and Shakhov (1993) solution for G_c in this paper was obtained by summing the multiple scattering series.

At early times, relatively few terms of the multiple scattering series are required to obtain a good approximation to the solution for G_c (see figures 3 and 4). The cut-offs in the plots of G_c as a function of t (figure 3) at $t = x/(v\mu_0)$ and at $t = x/(v\mu)$ are associated with G_1, the particles that have done a single scatter. These particles dominate G_c at early times. The plots of $\{G_n\}$ as functions of t have single maxima, with $G_n \to 0$ as $t \to |x - x_0|/v$ and as $t \to \infty$. The maxima occur at successively later times as n increases. At late times $t \gg |x - x_0|/v$, G_c may be approximated by the heat equation Green function (6.6). As t increases, it is necessary to use more terms of the multiple scattering series in order to obtain a good approximation to the total scattered Green function G_c (figures 6 and 8).

The multiple scattering approach can be applied to other transport phenomena governed by the Boltzmann equation (e.g. Kuhn 1979), such as radiative transfer (Chandrasekhar 1950) and neutron transport theory (Case and Zweifel 1967, Weinberg and Wigner 1958). In particular, it is of interest to use the multiple scattering approach to study the generalized BGK Boltzmann model of Kota (1994), in which there are two scattering timescales τ_1 and τ_2, where τ_1 describes particle scattering in the same hemisphere in velocity space (either the backward or forward hemisphere) and τ_2 describes scattering from one hemisphere to the other hemisphere. Chandrasekhar (1943) described stochastic transport phenomena in terms of an integral equation, in which the probability distribution ψ, at a particular phase space point is given by an integral over ψ at other points in phase space times a transition probability. Chandrasekhar's integral equation may be used to derive Fokker–Planck equations of the form (1.1) describing the pitch angle scattering of cosmic rays (Jokipii 1966). In principle, a multiple scattering approach associated with an iterative solution of Chandrasekhar's equation could be developed.

The relationship between path integral formulations of stochastic processes (Graham 1977, Zhang 1999), and Monte Carlo type methods associated with Itô's formulation of stochastic differential equations (e.g. Kloeden and Platen 1992, Krülls and Achterberg 1994) and multiple scattering is also of interest.

Acknowledgments

We acknowledge insightful remarks by the referees which improved the presentation. We acknowledge useful discussions with J Kota, A R Zakharian, J Y Lu and W K M Rice. The work of GMW was supported in part by NASA grant NAG5-5180. GPZ is supported in part at the BRI by NSF-DOE Award ATM-9713432, and in part by NASA grants NAG5-7796 and NAG5-6469.

Appendix A

In this appendix we sketch the derivation of the results (5.2) and (5.3) for the unscattered Green function G_0 and the Green function G_n for n-scatters.

Using the inversion formula (4.3) and expression (4.12) for $\tilde{G}_0$ yields the result

$$G_0 = \frac{\exp(-\bar{t})\delta(\mu-\mu_0)}{2\pi v\tau}\int_{c-\mathrm{i}\infty}^{c+\mathrm{i}\infty}\frac{\mathrm{d}\nu}{2\pi\mathrm{i}}\int_{-\infty}^{\infty}\mathrm{d}K\,\frac{\exp[\nu\bar{t}+\mathrm{i}K(\bar{x}-\bar{x}_0)]}{\nu+\mathrm{i}K\mu} \tag{A.1}$$

for the unscattered distribution G_0. Carrying out the inversion first with respect to ν in (A.1), taking into account the pole at $\nu = -\mathrm{i}K\mu$ yields

$$\begin{aligned} G_0 &= \frac{\exp(-\bar{t})\delta(\mu-\mu_0)}{v\tau}\int_{-\infty}^{\infty}\frac{\mathrm{d}K}{2\pi}\exp[\mathrm{i}K(\bar{x}-\bar{x}_0-\mu\bar{t})] \\ &\equiv \exp(-\bar{t})\delta(\mu-\mu_0)\delta(x-x_0-v\mu t) \end{aligned} \tag{A.2}$$

which is the Green function (5.2) for the unscattered particles.

To invert the transform (4.22) for $\tilde{G}_n$, the multi-valued function $a(K,\nu)$ in (4.10), namely

$$a(K,\nu) = \frac{\zeta}{2\mathrm{i}K} \qquad \zeta = \ln\left(\frac{K-\mathrm{i}\nu}{K+\mathrm{i}\nu}\right)+\mathrm{i}\pi \tag{A.3}$$

needs to be chosen so that $|a(K,\nu)| < 1$ on the integration path in the inversion formula (4.3) in order to ensure that the geometric series (4.23) for the total scattered distribution converges. In (4.3) we carry out the integration first with respect to K, keeping s (or ν) fixed. We choose the branch cut for ζ in (A.3) to consist of two disjoint segments of the $\mathrm{Im}\,(K)$ axis with $|\mathrm{Im}\,(K)| > \nu$, where $K = \pm\mathrm{i}\nu$ are the location of the branch points. In principle, there could be an extra phase factor of $2n\pi\mathrm{i}$ to ζ in (A.3) (n integer), but in fact it is necesssary to choose $n = 0$, in order to ensure $|a(K,\nu)| < 1$ on the $\mathrm{Re}\,(K)$ axis. One can show $\lim_{K\to 0} a(K,\nu) = 1/\nu$, where $\nu = 1+s\tau$; $|a(K,\nu)| \to 0$ as $|K| \to \infty$. On the branch cut

$$K = \mathrm{i}\nu/p \qquad |p| \leqslant 1. \tag{A.4}$$

On either side of the branch cut,

$$\zeta \to \begin{cases} m(p)+\mathrm{i}\pi & \text{if} \quad K = \mathrm{i}\nu/p+\epsilon \\ m(p)-\mathrm{i}\pi & \text{if} \quad K = \mathrm{i}\nu/p-\epsilon \end{cases} \tag{A.5}$$

where $\epsilon \downarrow 0$, and $m(p) = \ln|(1-p)/(1+p)|$. From (4.22) $\tilde{G}_n$ has poles located on the branch cut at

$$K = K_\mu = \mathrm{i}\frac{\nu}{\mu} \qquad \text{and} \qquad K = K_{\mu_0} = \mathrm{i}\frac{\nu}{\mu_0} \tag{A.6}$$

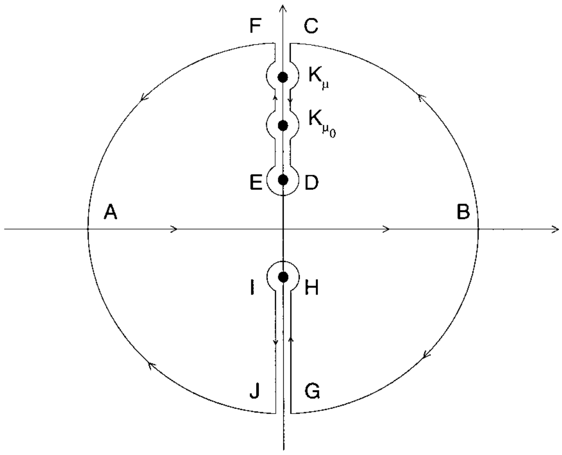

Figure 9. Contours in the complex K-plane used in the inversion of the transform (4.22) for $\tilde{G}_n$, using the inversion formula (4.3). For $\bar{x} > \bar{x}_0$ the contour AB is closed in the Im $(K) > 0$ half plane, but if $\bar{x}_0 > \bar{x}$, the contour is closed in the lower half K-plane (Im $(K) < 0$). The branch points for the complex function ζ occur at points D and H where $K = \pm \mathrm{i}\nu$, and the branch cut is along the Im (K) axis in the region $|\mathrm{Im}\,(K)| > \nu$. The integrand has poles at $K = K_\mu = \mathrm{i}\nu/\mu$ and $K = K_{\mu_0} = \mathrm{i}\nu/\mu_0$ located on the branch cut (in the figure $0 < \mu < \mu_0 < 1$ has been assumed).

that need to be taken into account when inverting $\tilde{G}_n$ using (4.3). The integration contour used in (4.3) when inverting $\tilde{G}_n$ is illustrated in figure 9. Closing the contour in the Im $(K) > 0$ half plane if $x - x_0 > 0$, and in the lower half plane Im $(K) < 0$ if $x - x_0 < 0$, and using Cauchy's theorem we obtain

$$G_n = \frac{\exp(-\bar{t})}{2\pi \mathrm{i}\tau} \int_{c-\mathrm{i}\infty}^{c+\mathrm{i}\infty} \mathrm{d}\nu \exp(\nu\bar{t}) \tilde{G}_n(\bar{x}, \nu, \mu, \mu_0) \tag{A.7}$$

where

$$\begin{aligned} \tilde{G}_n = \frac{\mathrm{i}}{4\pi \upsilon \nu^n} \!\!\!\!\!\!\!\; \int_{-1}^{1} \frac{\mathrm{d}p}{(p-\mu)(p-\mu_0)} \Bigg\{ & \exp[-\nu(\bar{x}-\bar{x}_0)/p] \left(-\frac{1}{2}p\right)^{n-1} \\ & \times([m(p)+\mathrm{i}\pi]^{n-1} - [m(p)-\mathrm{i}\pi]^{n-1}) \\ & \times[H(\bar{x}-\bar{x}_0)H(p) - H(\bar{x}_0-\bar{x})H(-p)] \Bigg\} \\ & + \frac{F_n(\bar{x}, \bar{x}_0, \nu; \mu)}{\mu-\mu_0} [H(\bar{x}-\bar{x}_0)H(\mu) - H(\bar{x}_0-\bar{x})H(-\mu)] \\ & - \frac{F_n(\bar{x}, \bar{x}_0, \nu; \mu_0)}{\mu-\mu_0} [H(\bar{x}-\bar{x}_0)H(\mu_0) - H(\bar{x}_0-\bar{x})H(-\mu_0)] \end{aligned} \tag{A.8}$$

and

$$F_n(\bar{x}, \bar{x}_0, \nu; \mu) = \frac{1}{2\upsilon\nu^n} \exp[-\nu(\bar{x}-\bar{x}_0)/\mu] \left(-\frac{1}{2}\mu\right)^{n-1} \mathrm{Re}\,([m(\mu)+\mathrm{i}\pi]^{n-1}) \tag{A.9}$$

(note $F_n(\bar{x}, \bar{x}_0, \nu; \mu_0)$ is obtained by replacing $\mu \to \mu_0$ in (A.9)). The CPV integral in (A.8) arises from integrating along the branch cut, and the F_n terms are due to the poles (A.6).

Using the inverse Laplace transform

$$\frac{1}{2\pi \mathrm{i}} \int_{c-\mathrm{i}\infty}^{c+\mathrm{i}\infty} \mathrm{d}\nu \frac{\exp(\nu\lambda)}{\nu^n} = \frac{\lambda^{n-1}}{(n-1)!} H(\lambda) \tag{A.10}$$

to carry out the inverse Laplace transform (A.7) yields the results (5.3)–(5.8) for G_n.

Appendix B

In this appendix we prove the identity (5.17), which links the multiple scattering decomposition (5.1) for the Green function G_c to the Fedorov and Shakhov (1993) solution form (5.9). First note that the right-hand side of (5.17), (which we denote by G_d) may be written in the alternative form:

$$
\begin{aligned}
G_d &= \frac{1}{2\pi v\tau}\int_0^{\frac{\pi}{2}} \mathrm{d}K \exp[(K\cot K-1)\bar{t}] \\
&\quad\times \frac{\{\cos(Ky)[\cos^2 K - \mu\mu_0 \sin^2 K] + \sin(Ky)\sin K\cos K(\mu+\mu_0)]\}}{(\cos^2 K + \mu_0^2\sin^2 K)(\cos^2 K + \mu^2\sin^2 K)} \\
&= \frac{1}{4\pi v\tau}\int_{-\frac{\pi}{2}}^{\frac{\pi}{2}} \mathrm{d}K \frac{K^2}{\sin^2 K}\left(\frac{\exp[(\nu-1)\bar{t}+\mathrm{i}Ky]}{(\nu+\mathrm{i}K\mu)(\nu+\mathrm{i}K\mu_0)}\right)_{\nu=K\cot K}. \qquad \text{(B.1)}
\end{aligned}
$$

Note that the second form of G_d in (B.1) is a superposition of diffusive eigenmodes of the form (4.16), associated with the resonant manifold $\nu = K\cot K$.

To prove (5.17) we consider first the case $y = \bar{x} - \bar{x}_0 > 0$. By making a change of integration variable of the form

$$w = \exp(\mathrm{i}K) \qquad \text{(B.2)}$$

in (B.1) we obtain

$$G_d = \frac{\exp(-\bar{t})H(y)}{\mathrm{i}\pi v\tau(1+\mu)(1+\mu_0)}\int_{\mathcal{C}} \mathrm{d}w \frac{w\exp\{[y-\bar{t}(1+w^2)/(1-w^2)]\ln w\}}{(w+\mathrm{i}w_{\mu_0})(w-\mathrm{i}w_{\mu_0})(w+\mathrm{i}w_\mu)(w-\mathrm{i}w_\mu)} \qquad \text{(B.3)}$$

where

$$w_\mu = \left(\frac{1-\mu}{1+\mu}\right)^{\frac{1}{2}} \qquad w_{\mu_0} = \left(\frac{1-\mu_0}{1+\mu_0}\right)^{\frac{1}{2}}. \qquad \text{(B.4)}$$

In (B.3), the contour $\mathcal{C}$ in the complex w-plane consists of a semi-circular arc of unit radius ($|w| = 1$) in the Re $(w) > 0$ half plane with endpoints at $w = \pm\mathrm{i}$. A schematic of the contour $\mathcal{C}$ and the pole locations at $w = \pm\mathrm{i}w_{\mu_0}$ and at $w = \pm\mathrm{i}w_\mu$ are displayed in figure 10.

For $y = \bar{x} - \bar{x}_0 < 0$, we use an equivalent integral representation for G_d, by using the integration variable

$$\tilde{w} = \exp(-\mathrm{i}K) \qquad \text{(B.5)}$$

in (B.1) to obtain

$$G_d = \frac{\exp(-\bar{t})H(y)}{\mathrm{i}\pi v\tau(1-\mu)(1-\mu_0)}\int_{\tilde{\mathcal{C}}} \mathrm{d}\tilde{w} \frac{\tilde{w}\exp\{[-y-\bar{t}(1+\tilde{w}^2)/(1-\tilde{w}^2)]\ln\tilde{w}\}}{(\tilde{w}+\mathrm{i}\tilde{w}_{\mu_0})(\tilde{w}-\mathrm{i}\tilde{w}_{\mu_0})(\tilde{w}+\mathrm{i}\tilde{w}_\mu)(\tilde{w}-\mathrm{i}\tilde{w}_\mu)} \qquad \text{(B.6)}$$

where

$$\tilde{w}_\mu = \left(\frac{1+\mu}{1-\mu}\right)^{\frac{1}{2}} \qquad \tilde{w}_{\mu_0} = \left(\frac{1+\mu_0}{1-\mu_0}\right)^{\frac{1}{2}}. \qquad \text{(B.7)}$$

and the contour $\tilde{\mathcal{C}}$ in the complex $\tilde{w}$-plane is essentially of the same form as in figure 10, except that the poles now occur at $\tilde{w} = \pm\mathrm{i}\tilde{w}_{\mu_0}$ and at $\tilde{w} = \pm\mathrm{i}\tilde{w}_\mu$.

If $y = \bar{x} - \bar{x}_0 > 0$, the expression (B.3) is used for G_d, and the contour $\mathcal{C}$ (i.e. ABC) is closed by the path COA in figure 10. If $y = \bar{x} - \bar{x}_0 > \bar{t}$, the integrand is bounded at $w = 0$. If $\bar{t} > \bar{x} - \bar{x}_0$ (i.e. the causal case for which $G_c \neq 0$), the integrand (B.3) diverges as $w \to 0$. However, if the exponential function in (B.3) is expanded using the Taylor series for

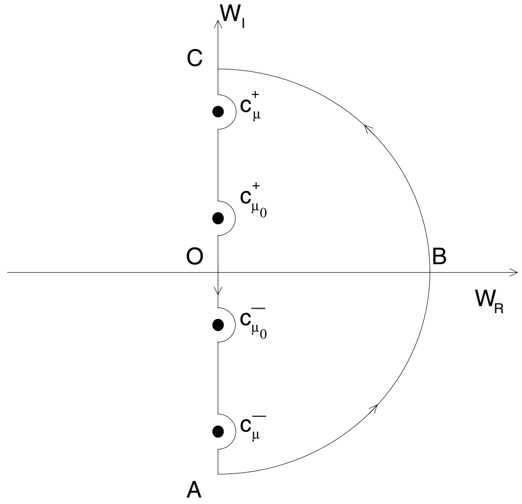

Figure 10. Contour path ABCOA in the complex $w = w_R + \mathrm{i}w_I$-plane used in transforming the contour integral (B.3). The contour $\mathcal{C}$ in (B.3) consists of the semi-circular arc ABC in $w_R > 0$, with centre $w = 0$, and radius $|w| = 1$. The small semi-circular arcs $C_\mu^\pm$ and $C_{\mu_0}^\pm$ are indentations around the poles at $w = \pm\mathrm{i}w_\mu$ and $w = \pm\mathrm{i}w_{\mu_0}$ ($0 < \mu < 1$ and $0 < \mu_0 < 1$ in the diagram). If $-1 < \mu < 0$, the poles $w = \pm\mathrm{i}w_\mu$ lie on the w_I-axis, in the region $|w_I| > 1$, and similarly for the location of the poles $w = \pm\mathrm{i}w_{\mu_0}$.

the exponential function, each individual term in the series results in a bounded integrand at $w = 0$, since

$$\lim_{w\to 0} w[\ln(w)]^n = 0 \tag{B.8}$$

for each positive integer n. A similar strategy can be used in the case $y = \bar{x} - \bar{x}_0 < 0$, where the divergence of the exponential function in (B.6) as $\tilde{w} \to 0$ for $\bar{t} > \bar{x}_0 - \bar{x}$, may be dealt with in a similar fashion. Using Cauchy's theorem for the closed contour, we obtain

$$G_d = \sum_{n=0}^{\infty} I_n \tag{B.9}$$

where

$$\begin{aligned} I_n = &-\frac{\exp(-\bar{t})H(y)}{\mathrm{i}\pi v\tau(1+\mu)(1+\mu_0)n!}\int_{\mathrm{COA}} \mathrm{d}w \frac{w\{[y - \bar{t}(1+w^2)/(1-w^2)]\ln w\}^n}{(w+\mathrm{i}w_\mu)(w-\mathrm{i}w_\mu)(w+\mathrm{i}w_{\mu_0})(w-\mathrm{i}w_{\mu_0})} \\ &-\frac{\exp(-\bar{t})H(-y)}{\mathrm{i}\pi v\tau(1-\mu)(1-\mu_0)n!} \\ &\times \int_{\tilde{\mathrm{C}}\tilde{\mathrm{O}}\tilde{\mathrm{A}}} \mathrm{d}\tilde{w} \frac{\tilde{w}\{[-y - \bar{t}(1+\tilde{w}^2)/(1-\tilde{w}^2)]\ln \tilde{w}\}^n}{(\tilde{w}+\mathrm{i}\tilde{w}_\mu)(\tilde{w}-\mathrm{i}\tilde{w}_\mu)(\tilde{w}+\mathrm{i}\tilde{w}_{\mu_0})(\tilde{w}-\mathrm{i}\tilde{w}_{\mu_0})}. \end{aligned} \tag{B.10}$$

Taking into account the indentations around the poles on the path COA in the complex w-plane (and similarly for the corresponding path $\tilde{\mathrm{C}}\tilde{\mathrm{O}}\tilde{\mathrm{A}}$ in the $\tilde{w}$-plane), we find

$$\begin{aligned} I_{n-1} = \frac{\exp(-\bar{t})}{2v\tau(\mu-\mu_0)}\bigg[&-\frac{1}{\pi}\fint_{-1}^{1} \mathrm{d}p\left(\frac{1}{p-\mu} - \frac{1}{p-\mu_0}\right)\hat{V}_n^-(y,\bar{t},p) \\ &\times[H(y)H(p) - H(-y)H(-p)] \\ &+\hat{V}_n^+(y,\bar{t},\mu)[H(y)H(\mu) - H(-y)H(-\mu)] \end{aligned}$$

$$-\hat{V}_n^{+}(y,\bar{t},\mu_0)[H(y)H(\mu_0)-H(-y)H(-\mu_0)]\Bigg] \tag{B.11}$$

where $y=\bar{x}-\bar{x}_0$ and $\hat{V}_n^{\pm}$ are defined in (5.6) and (5.7).

Using Cauchy's theorem for the closed path COABC in the complex w-plane in figure 10 for the case $y>0$, and the corresponding path $\tilde{\mathrm{C}}\tilde{\mathrm{O}}\tilde{\mathrm{A}}\tilde{\mathrm{B}}\tilde{\mathrm{C}}$ in the $\tilde{w}$-plane if $y<0$, the integral (B.10) may be written in the alternative form

$$I_{n-1}=\frac{\exp(-\bar{t})}{2\pi v\tau}\frac{1}{(n-1)!}\int_0^{\frac{\pi}{2}}\mathrm{d}K\,\mathrm{Re}\left(\frac{(\mathrm{i}Ky+K\cot K\bar{t})^{n-1}}{(\cos K+\mathrm{i}\mu\sin K)(\cos K+\mathrm{i}\mu_0\sin K)}\right). \tag{B.12}$$

The form (B.12) is useful in determining the behaviour of the Green function G_n at late times (see (5.18) et seq.).

Using the result (B.11) in (B.9), and summing over n yields the result

$$\begin{aligned}G_d=&-\frac{\exp(-\bar{t})}{2\pi v\tau}\sum_{n=1}^{\infty}\int_{-1}^{1}\frac{\mathrm{d}p}{(p-\mu)(p-\mu_0)}\mathrm{Im}\left\{\frac{((y-p\bar{t})[m(p)+\mathrm{i}\pi])^n}{2^n n!}\right\}\\&\times[H(y)H(p)-H(-y)H(-p)]\\&+\frac{\exp(-\bar{t})}{2v\tau(\mu-\mu_0)}\left\{\left|\frac{1-\mu}{1+\mu}\right|^{\frac{1}{2}(y-\mu\bar{t})}\cos\left[\frac{1}{2}\pi(y-\mu\bar{t})\right]\right.\\&\times[H(y)H(\mu)-H(-y)H(-\mu)]\\&-\left|\frac{1-\mu_0}{1+\mu_0}\right|^{\frac{1}{2}(y-\mu_0\bar{t})}\cos\left[\frac{1}{2}\pi(y-\mu_0\bar{t})\right]\\&\left.\times[H(y)H(\mu_0)-H(-y)H(-\mu_0)]\right\}.\end{aligned} \tag{B.13}$$

This establishes the identity (5.17).

Appendix C

In this appendix we discuss the late time behaviour of G_c and $\langle f\rangle$. We first discuss the resonant manifold or dispersion equation (4.14) for the diffusive type eigenmodes, and its relation to the diffusion equation and telegraph equation approximations. We also derive the approximate Green function (6.6) for G_c applicable for late times t.

First note (see also Kota 1994), that the resonant manifold (4.14) for the diffusive eigenmodes, namely

$$\nu\equiv 1+s\tau=K\cot K\qquad |K|<\tfrac{1}{2}\pi \tag{C.1}$$

for small K may be expanded as

$$s\tau=-\frac{K^2}{3}-\frac{K^4}{45}+\mathrm{O}(K^6) \tag{C.2}$$

(Abramowitz and Stegun 1965, p 75, formula 4.3.70). Neglecting $\mathrm{O}(K^4)$ terms in (C.2), the dispersion relation (C.2) in real (x,t)-space implies that the diffusive eigenmodes g in (4.16), at late times ($s\to 0$, $K\to 0$, $t\to\infty$) satisfy the diffusion equation

$$g_t-\kappa g_{xx}=0 \tag{C.3}$$

where $\kappa=\frac{1}{3}v^2\tau$. If one retains the $\mathrm{O}(K^4)$ term in (C.2), and uses the lowest-order balance $s\tau\sim\frac{1}{3}K^2$, then at the next order (C.2) can be approximated by

$$s\tau=-\frac{K^2}{3}-\frac{s^2\tau^2}{5}+\mathrm{O}(K^4). \tag{C.4}$$

The dispersion equation (C.4) in (x, t)-space is equivalent to the telegraph equation for $\langle f\rangle$ obtained by Gombosi *et al* (1993) (see also, Kota 1994).

The Green function (6.6) can be derived by using the approximate dispersion relation $s\tau \simeq -\frac{1}{3}K^2$ appropriate for late times and directly invert the transform (4.13). An alternative, simpler procedure is to note that at late times the Fedorov–Shakhov solution (5.9) and (5.10) is dominated by the diffusive eigenmodes (the integral from $K = 0$ to $\frac{1}{2}\pi$). Thus at late times

$$G_c \simeq G_d = \frac{1}{2\pi v\tau}\int_0^{\frac{\pi}{2}} \mathrm{d}K \exp[(K\cot K - 1)\bar{t}] \times \frac{\cos(Ky)[\cos^2 K - \mu\mu_0\sin^2 K] + \sin(Ky)\sin K\cos K(\mu + \mu_0)}{(\cos^2 K + \mu_0^2\sin^2 K)(\cos^2 K + \mu^2\sin^2 K)}. \tag{C.5}$$

For large times $\bar{t}$, the integral (C.5) is dominated by the value of the integrand in the neighbourhood of $K = 0$, so that

$$s\tau \equiv K\cot K - 1 \simeq -\frac{K^2}{3} \tag{C.6}$$

$\cos K \simeq 1$, $\sin K \simeq 0$ may be used near $K = 0$. Using these approximations, and extending the upper limit on the integral at $K = \frac{1}{2}\pi$ to $K = \infty$ in (C.5) yields the approximation

$$G_c \simeq \frac{1}{2\pi v\tau}\int_0^{\infty} \mathrm{d}K \exp\left(-\frac{K^2\bar{t}}{3}\right)\cos(Ky) \equiv \frac{1}{4\pi v\tau}\int_{-\infty}^{\infty} \mathrm{d}K \exp\left(-\frac{K^2\bar{t}}{3} + \mathrm{i}Ky\right). \tag{C.7}$$

It is straightforward to show that (C.7) is equivalent to the diffusion equation Green function (6.6).

References

Abramowitz M and Stegun I A 1965 *Handbook of Mathematical Functions* (New York: Dover)

Berezhko E G and Krymsky G F 1981 *Sov. Astron. Lett.* **7** 352

Berezhko E G, Yelshin V K, Krymsky G F and Romaschenko Yu A 1983 *Proc. 18th Int. Cosmic Ray Conf. (Bangalore, India)* vol 2 p 259

Case K M and Zweifel P F 1967 *Linear Transport Theory* (Reading MA: Addison-Wesley)

Chandrasekhar S 1943 *Rev. Mod. Phys.* **15** 1

——1950 *Radiative Transfer Theory* (Oxford: Clarendon)

Dolginov A Z and Toptygin I N 1967 *Geomagn. Aeron.* **7** 785

Earl J A 1974a *Astrophys. J.* **188** 379

——1974b *Astrophys. J.* **193** 231

——1989 *Astrophys. J.* **343** 936

——1993 *Astrophys. J.* **425** 331

Earl J A, Jokipii J R and Morfill G E 1988 *Astrophys. J. Lett.* **331** L91

Fedorov Yu I and Shakhov B A 1993 *Proc. 23rd Int. Cosmic Ray Conf. (Calgary)* vol 3 p 215

Fedorov Yu I, Shakhov B A and Stehlik M 1995 *Astron. Astrophys.* **302** 623–34

Fedorov Yu I, Kyzyurov Yu V, Nosov S F and Shakhov B A 1996 *Ann. Geophysicae* **14** 1016–8

Fisk L A and Axford W I 1969 *Solar Phys.* **7** 486

Gleeson L J and Axford W I 1967 *Astrophys. J. Lett.* **149** L115

Gombosi T A, Jokipii J R, Kota J, Lorencz K and Williams L L 1993 *Astrophys. J.* **403** 377

Graham R 1977 *Z. Phys.* B **26** 281

Hasselmann K and Wibberenz G 1970 *Astrophys. J.* **162** 1049

Jokipii J R 1966 *Astrophys. J.* **159** 61

Jokipii J R, Levy E H and Hubbard W B 1977 *Astrophys. J.* **213** 861

Kirk J G and Schneider P 1987a *Astrophys. J.* **315** 425

——1987b *Astrophys. J.* **322** 256
Kloeden P E and Platen E 1992 *Numerical Solution of Stochastic Differential Equations* (New York: Springer)
Kota J 1994 *Astrophys. J.* **427** 1035
Kota J, Merényi E, Jokipii J R, Kopriva D A, Gombosi T A and Owens A J 1982 *Astrophys. J.* **254** 398
Krülls W and Achterberg A 1994 *Astron. Astrophys.* **286** 314
Kuhn S 1979 *Mathematical Methods of Plasma Physics* vol 20 (Frankfurt am Main: Peter D Lang GmbH) p 99
Lin R P 1970 *J. Geophys. Res.* **75** 2583
Morse P M and Feshbach H 1953 *Methods of Theoretical Physics* vol 1 (New York: McGraw-Hill)
Ng C K and Wong K Y 1979 *Proc. 16th Int. Conf. on Cosmic Ray (Kyoto)* vol 5 p 252
Parker E N 1965 *Planet. Space. Sci.* **13** 9
Pauls L H, Burger A and Bieber J W 1993 *Proc. 23rd Int. Conf. on Cosmic Ray (Calgary)* vol 3 p 183
Ruffolo D 1991 *Astrophys. J.* **382** 688
Skilling J 1975 *Mon. Not. R. Astron. Soc.* **172** 557
Webb G M 1989 *Astrophys. J.* **340** 1112
Webb G M, Zank G P, Pantazopoulou M and Zakharian A R 1999 *Proc. 26th Int. Conf. on Cosmic Ray (Salt Lake City, Utah)* vol 6, pp 351–4
Weinberg A M and Wigner E P 1958 *The Physical Theory of Neutron Chain Reactors* (Chicago, IL: University of Chicago Press)
Zank G P, Lu J Y, Rice W K M and Webb G M 1999 *Proc. 26th Int. Conf. on Cosmic Ray (Salt Lake City, Utah)* vol 6, pp 312–5
Zhang M 1999 *Astrophys. J.* **510** 715